THE PUBLISHING HOUSE
OF THE ROMANIAN ACADEMY

PROCEEDINGS OF THE ROMANIAN ACADEMY, Series A,
Volume 19, Number 1/2018, pp. 61–68

SYMMETRY BREAKING OF SOLITONS IN PT-SYMMETRIC POTENTIALS WITH COMPETING CUBIC-QUINTIC NONLINEARITY

Pengfei LI [1], Dumitru MIHALACHE [2]

[1] Taiyuan Normal University, Department of Physics, Taiyuan, 030031, China
[2] "Horia Hulubei" National Institute of Physics and Nuclear Engineering, Magurele, Bucharest, RO-077125, Romania
Corresponding author: Pengfei LI, E-mail: lpf281888@gmail.com

Abstract. Symmetry breaking of solitons in optical waveguides with competing cubic-quintic nonlinearity and parity-time (PT)-symmetric complex-valued external potentials is investigated. This symmetry breaking can only exist in a special class of PT-symmetric potentials. It is shown that the branches corresponding to asymmetric soliton solutions bifurcate from the base branches of PT-symmetric fundamental soliton and the excited state soliton solutions with the increasing of input power. The effect of the modulation strength of PT-symmetric potential on the structure of eigenvalue spectra diagrams of the symmetric and asymmetric soliton solutions is investigated. The stability of the symmetric and asymmetric soliton solutions are comprehensively analyzed by employing linear stability analysis and the different instability scenarios of solitons have also been revealed by using directly numerical simulations.

Key words: competing cubic-quintic nonlinearity, PT-symmetry breaking, asymmetric soliton.

1. INTRODUCTION

Parity-time (PT)-symmetric systems have attracted a growing interest in the past several years. These systems are non-Hermitian due to the presence of gain and loss, which are delicately balanced due to the complex potential satisfies $U\left(\xi\right)=U^{*}\left(-\xi\right)$, where asterisk denotes the complex conjugation. Thus the PT-symmetry requires that the real part of the complex-valued potential $U\left(\xi\right)$ must be an even function of the position ξ, whereas the imaginary part must be an odd function. One of the key properties for PT-symmetric systems is that there can exist all real eigenvalue spectra, as demonstrated twenty years ago in a seminal work by Bender and Boettcher in the quantum mechanics framework [1–3].

The concept of PT-symmetry has gone far beyond the quantum physics, such as optics and photonics [4, 5], Bose-Einstein condensates [6], plasmonic waveguides and metamaterials [7–9], superconductivity [10], etc. In the optics context, the real part of the complex-valued potential stands for the spatial distribution of the refractive index and the imaginary part stands for the balanced gain and loss of optical waveguides. Thus one can construct an optical analog of PT-symmetric quantum mechanics, which was firstly investigated theoretically [4, 11] and later realized in the paraxial regime [12–14]. Furthermore, PT-symmetric soliton solutions and light transmission have been widely explored in nonlinear regimes with linear complex-valued PT-symmetric potentials. A variety of optical solitons have been studied, including bright solitons, gap solitons, Bragg solitons, and dark solitons [15–28].

Recently, the symmetry breaking of solitons in PT-symmetric potentials has aroused great attention. It has been shown that this symmetry breaking cannot occur in generic PT-symmetric potentials. But for a special class of PT-symmetric potentials $U\left(\xi\right)=g^{2}\left(\xi\right)+\alpha g\left(\xi\right)+\mathrm{i}\mathrm{d}g\left(\xi\right)/\mathrm{d}\xi$ with a real constant α and an arbitrary real even function $g\left(\xi\right)$, a family of stable PT-symmetry-breaking solitons with real eigenvalue spectra have been found [29]. For this type of potentials, a precondition of the existence of non-PT-symmetric (asymmetric) solitons is miraculously satisfied [30]. These asymmetric solitons bifurcate out from the base branch of PT-symmetric solitons when the soliton power exceeds a certain threshold [31].

In this paper, we will carry out a detailed investigation of symmetry breaking of solitons in PT-symmetric potentials with competing cubic-quintic (CQ) nonlinearity and study the key features of both symmetric and asymmetric solitons. The paper is organized as follows. In Sec. 2, the governing model is introduced. In Sec. 3, we show the symmetry breaking bifurcation of eigenvalue spectrum and present asymmetric and symmetric soliton solutions. The dependence of the nonlinear propagation constants on the input power and the modulation strength of the complex-valued potential are also discussed. In Sec. 4, we analyze systematically the stability of asymmetric and symmetric solutions, and their nonlinear evolution dynamics is studied by performing direct numerical simulations. Finally, we conclude the paper in Sec. 5.

2. THE GOVERNING MODEL

Optical wave propagation in a planar graded-index waveguide with CQ nonlinearity is governed by the following (1+1)-dimensional paraxial wave equation

$$\mathrm{i}\frac{\partial A}{\partial z}+\frac{1}{2k_0}\frac{\partial^2 A}{\partial x^2}+\frac{k_0\left[F(x)-n_0\right]}{n_0}A+\frac{k_0}{n_0}n_2|A|^2A+\frac{k_0}{n_0}n_4|A|^4A=0, \tag{1}$$

where $A(z,x)$ is the optical field envelope function, $k_0=2\pi n_0/\lambda$ is the wavenumber with λ and n_0 being the wavelength of the optical source and the background refractive index, respectively. Here, $F(x)=F_R(x)+iF_I(x)$ is a complex-valued function, in which the real part represents the linear refractive index distribution and the imaginary part stands for gain and loss; n_2 and n_4 are the cubic and quintic nonlinear parameters, respectively. Introducing the transformations $\psi(\zeta,\xi)=\sqrt{|n_4|/|n_2|}A(z,x)$, $\xi=k_0n_2\sqrt{2/(n_0|n_4|)}x$, and $\zeta=k_0n_2^2/(n_0|n_4|)z$, Eq. (1) can be rewritten in a dimensionless form

$$\mathrm{i}\frac{\partial\psi}{\partial\zeta}+\frac{\partial^2\psi}{\partial\xi^2}+U(\xi)\psi+\sigma_1|\psi|^2\psi+\sigma_2|\psi|^4\psi=0. \tag{2}$$

Here $\sigma_1=n_2/|n_2|=\pm1$ and $\sigma_2=n_4/|n_4|=\pm1$, where ±1 corresponds to self-focusing $(+)$ or self-defocusing $(-)$ situations, respectively. The normalized potential is $U(\xi)\equiv V(\xi)+iW(\xi)$ with $V(\xi)=|n_4|\left[F_R(x)-n_0\right]/n_2^2$ and $W(\xi)=|n_4|F_I(x)/n_2^2$, which are required to be even and odd functions, respectively, for PT-symmetric nonlinear optical waveguides. In this model, we consider a special class of PT-symmetric potentials $V(\xi)=g^2(\xi)+\alpha g(\xi)$ and $W(\xi)=\mathrm{d}g(\xi)/\mathrm{d}\xi$ with $g(\xi)$ being an arbitrary real and even function and α being an arbitrary real constant. The functions $g(\xi)$ can be taken as localized double-hump functions or as periodic functions. If $\sigma_2=0$, it has been shown that the eigenvalue spectrum of asymmetric soliton can bifurcate from the base branch of symmetric solitons with the increasing of soliton power, and the existence of stable PT-symmetry-breaking solitons was proved [29]. These results were extended to two-dimensional potentials [31, 32]. Subsequently, the effects of the soliton power, the separation between the two humps of the potential, the width and the modulation strength of the potential on the structure of the linear stability eigenvalue spectrum was studied [33]. To analyze the symmetry breaking of solitons in PT-symmetric potentials of Eq. (2), we need to assume the stationary solutions in the form $\psi(\xi)=\phi(\xi)\mathrm{e}^{\mathrm{i}\beta\zeta}$, where $\phi(\xi)$ is a complex-valued function and β is the corresponding nonlinear propagation constant. Substitution into Eq. (2) yields

$$\frac{\partial^2\phi(\xi)}{\partial\xi^2}+U(\xi)\phi(\xi)+\sigma_1|\phi|(\xi)^2\phi(\xi)+\sigma_2|\phi(\xi)|^4\phi(\xi)-\beta\phi(\xi)=0. \tag{3}$$

Here, we take $g(\xi)$ in the form

$$g(\xi)=W_0\left[\operatorname{sech}\left(\frac{\xi+\xi_0}{\chi_0}\right)+\operatorname{sech}\left(\frac{\xi-\xi_0}{\chi_0}\right)\right], \tag{4}$$

where χ_0 and ξ_0 are related to the width and the separation between the two humps of the potential, respectively, and W_0 represents the modulation strength of the complex potential.

3. STATIONARY SOLITON SOLUTIONS AND SYMMETRIY-BREAKING BIFURCATIONS

In this Section, we will explore symmetry-breaking bifurcations and the existence of stationary soliton solutions including the symmetric and asymmetric waveforms. Here, we consider the competing CQ nonlinearity, i.e., $\sigma_1=+1$ and $\sigma_2=-1$ in Eq. (3). The complex PT-symmetric potential $U(\xi)$ is shown in Fig. 1a with $\xi_0=2$, $\chi_0=1$, and $W_0=2$. The numerical results show that there exist fundamental symmetric soliton solutions as well as the excited state soliton solutions. The eigenvalue spectra of two kinds of asymmetric soliton solutions bifurcate from the corresponding two types of the base branches of the symmetric soliton solutions, by varying the soliton power $P=\int_{-\infty}^{+\infty}|\psi|^2\,\mathrm{d}\xi$.

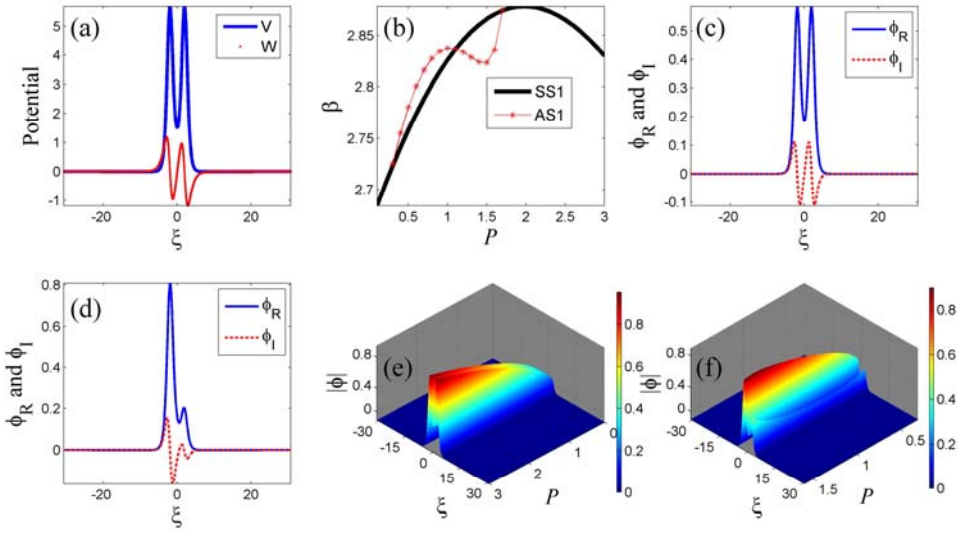

Fig. 1 – Bifurcation of eigenvalue spectrum and the corresponding symmetric and asymmetric soliton solutions: a) real (blue solid curve) and imaginary (red dotted curve) components of the potential; b) the propagation constant versus the soliton power for symmetric fundamental soliton solutions (black solid curve) and asymmetric (red curve) solutions; c) and d) distributions of fundamental symmetric and asymmetric solutions with the soliton power 1.1, where the blue solid and red dash-dotted curves represent the real and imaginary components, respectively; e) and f) Fundamental symmetric and asymmetric soliton solutions for different soliton powers.

In Fig. 1, we show the dependence of the propagation constant β on the soliton power P, i.e., the nonlinear eigenvalue spectrum curves $\beta=\beta(P)$ of symmetric and asymmetric soliton solutions. In Fig. 1b, the black thick solid curve and thin red curve with stars show the nonlinear eigenvalue spectra of the fundamental symmetric soliton solutions (SS1) and the corresponding fundamental asymmetric soliton solutions (AS1). For AS1, the eigenvalue spectrum begins to separate out when soliton power $P>0.3$ and bifurcates upward, then it crosses the base branch of SS1 at the point of $P=1.1$ and bifurcates downward. The eigenvalue spectrum of AS1 ceases at $P=1.7$. It is worth noting that SS1 and AS1 possess the same propagation constant and soliton power at the crossing point ($P=1.1$), so they constitute a pair of

degenerate nonlinear modes. This result is different from the case of PT-symmetric cubic nonlinearity model [29, 31–33]. We present these two degenerate soliton solutions at the point of $P=1.1$ in Fig. 1c and Fig. 1d, respectively. It is a natural result for the fundamental symmetric soliton solution that the complex-valued function satisfies $\phi(\xi)=\phi^*(-\xi)$ and possesses symmetric real profiles and antisymmetric imaginary ones, as shown in Fig. 1c. But for AS1 shown in Fig. 1d, the real and imaginary profiles are all asymmetric. Furthermore, the symmetric and asymmetric soliton solutions for the different powers are presented in Fig. 1e and Fig. 1f; one can see that the fundamental asymmetric soliton solutions can exist in the region $0.3<P<1.7$, as shown in Fig. 1f.

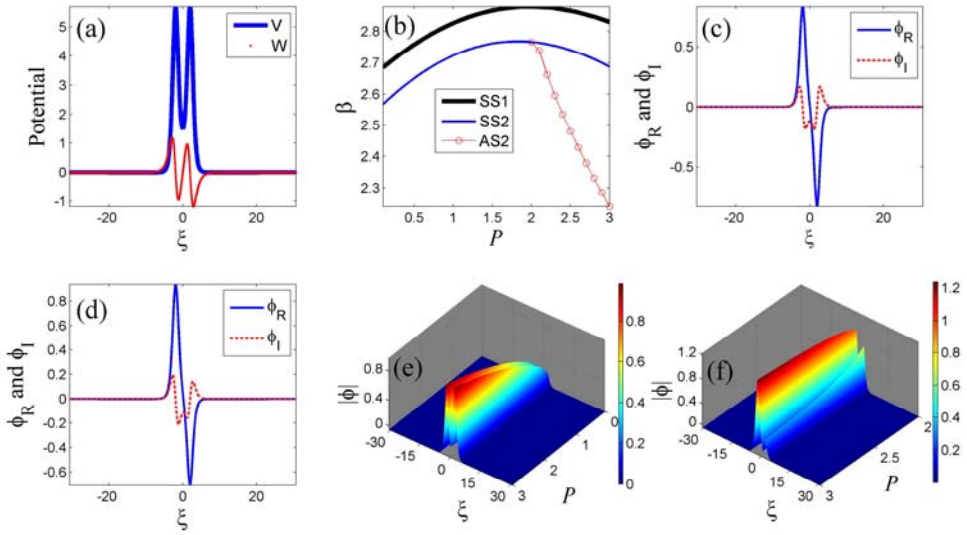

Fig. 2 – Bifurcation of eigenvalue spectrum for the excited states of symmetric soliton solutions and asymmetric soliton solutions: a) real (blue solid curve) and imaginary (red dotted curve) components of the potential with the same parameters as in Fig. 1; b) the propagation constant versus the soliton power for the fundamental symmetric soliton solutions (black thick solid curve), the excited state of symmetric soliton solution (blue thin solid curve) and the excited state of asymmetric (red circles curve) solution; c) and d) Distributions of the excited state for symmetric and asymmetric solutions with the soliton power 2.1, where the blue solid and red dash-dotted curves represent the real and imaginary components, respectively; e) and f) The excited state of symmetric and asymmetric soliton solutions for different soliton powers.

The results of numerical calculations show that there also exists another type of symmetric soliton solutions in Eq. (3), i.e., the excited state of symmetric soliton (SS2). By varying soliton power, the other eigenvalue spectrum of asymmetric soliton solutions (AS2) bifurcates from the SS2 branch. Here, the parameters of potential in Fig. 2a are the same as the Fig. 1. To present the second bifurcation phenomenon, the eigenvalue spectra of these two types of symmetric solitons (SS1 and SS2) are plotted in Fig. 2b with black thick solid curve and blue thin solid curve, respectively. One can see that the eigenvalue spectrum of AS2 bifurcates from the second branch of symmetric solutions. So the soliton's symmetry can be broken not only for the fundamental symmetric solitons but also for the excited state solitons. As an example, we show the distributions of the excited states for symmetric and asymmetric solitons at the power $P=2.1$. As shown in Fig. 2c and Fig. 2d, the blue solid and red dash-dotted curves represent the real and imaginary components of soliton solutions. Note that the SS2 solutions have the opposite symmetry, i.e., antisymmetric real profiles and symmetric imaginary ones. The excited state of symmetric soliton and the corresponding asymmetric soliton branch for different soliton powers are presented in Figs. 2e and 2f, respectively. The results show that the AS2 branch can exist in the region $2.0<P<3.0$.

To comprehensively analyze the features of the symmetry-breaking bifurcations, we also investigate the influence of the modulation strength of the complex potential on the eigenvalue spectra of the symmetric and asymmetric solutions. The range of the power P is chosen to vary from 0.1 to 3 for given χ_0 and ξ_0, the eigenvalue spectra of the symmetric and asymmetric solutions for both the fundamental and the excited state solitons are obtained by varying the parameter W_0. The results are summarized in Fig. 3. We find that

the propagation constant β is an increasing function of W_0, the values of the eigenvalue spectra of the fundamental symmetric and asymmetric soliton solutions are very close to each other, as shown in Fig. 3a. In Fig. 3b, the existence region of the fundamental asymmetric solitons is shown in the plane $P-W_0$; it is found that this region is enlarging with increasing of the modulation strength W_0. The eigenvalue spectra of the excited states for SS2 and AS2 are presented in Fig. 3c for different modulation strengths W_0; one can see the typical *fork-type* eigenvalue spectra structure due to the symmetry-breaking of SS2. This type of bifurcating structure is similar to the case of cubic nonlinearity [30]. The existence region of the excited states for AS2 is also plotted in Fig. 3d in plane of $P-W_0$. The results show that the existence region for AS2 is significantly reduced when the strength W_0 is decreased and vanishes at $W_0=1.4$, which is closely related to the stability of the symmetric soliton solutions, as to be discussed in the next Section.

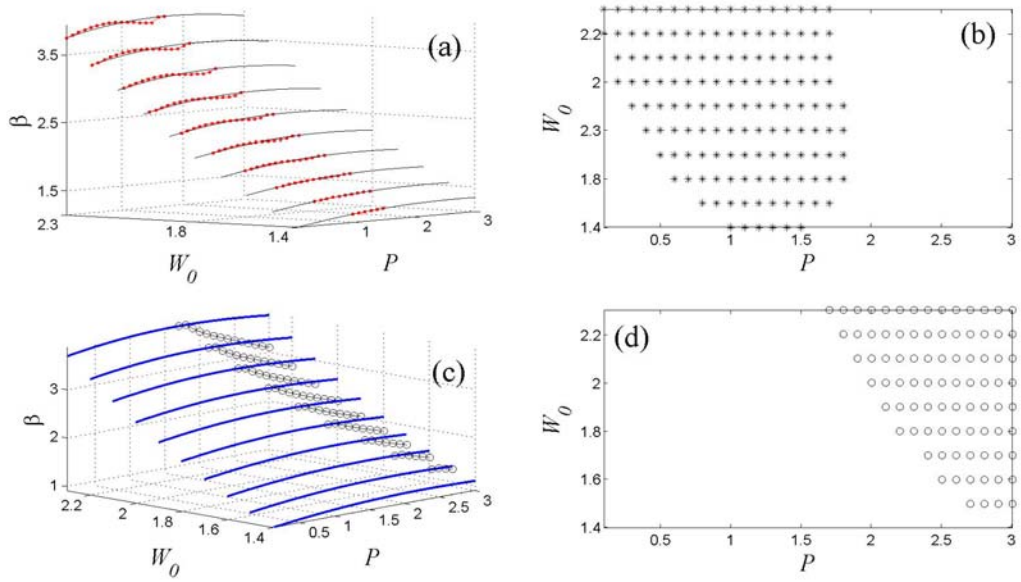

Fig. 3 – The eigenvalue spectra as a function of the power P for the symmetric and asymmetric solutions: a) the eigenvalue spectra of fundamental symmetric solitons (black solid curves) and asymmetric solitons (red squares) for different modulation strengths of the complex potential; b) the existence region of the fundamental asymmetric solitons (black stars); c) the eigenvalue spectra of the excited state of symmetric solitons (blue solid curves) and asymmetric solitons (black circles) solutions for different modulation strengths of the complex potential; d) the existence region of the excited state for asymmetric soliton solutions (black circles). Here, the soliton power ranges from 0.1 to 3, the modulation strength ranges from 1.4 to 2.3 and the other potential's parameters are the same as in Fig. 1.

4. LINEAR STABILITY ANALYSIS

In order to understand the stability features of these symmetric and asymmetric soliton solutions, we will address the linear stability analysis on these solutions. The corresponding evolution dynamics are investigated by direct numerical simulations. The linear stability analysis can be performed by adding a small perturbation to a known solution $\phi(\xi)$

$$\psi(\zeta,\xi)=\mathrm{e}^{\mathrm{i}\beta\zeta}\left[\phi(\xi)+u(\xi)\mathrm{e}^{\delta\zeta}+v^{*}(\xi)\mathrm{e}^{\delta^{*}\zeta}\right], \tag{5}$$

where $\phi(\xi)$ is the stationary solution with real propagation constant β, $u(\xi)$ and $v(\xi)$ are small perturbations with $|u|$, $|v|<<|\phi|$. Substituting Eq. (5) into Eq. (2) and keeping only the linear terms, we obtain the following linear eigenvalue problem

$$\mathrm{i}\begin{pmatrix} L_{11} & L_{12} \\ L_{21} & L_{22} \end{pmatrix}\begin{pmatrix} u \\ v \end{pmatrix} = \delta \begin{pmatrix} u \\ v \end{pmatrix}, \tag{6}$$

where $L_{11} = \mathrm{d}^2/\mathrm{d}\xi^2 + U - \beta + 2\sigma_1|\phi|^2 + 3\sigma_2|\phi|^4$, $L_{12} = \sigma_1|\phi|^2 + 2\sigma_2\phi^2|\phi|^2$, $L_{21} = -L_{12}^*$, $L_{22} = -L_{11}^*$, and δ is a complex eigenvalue of the linear problem (6). The positive real part of complex eigenvalue can be used to measure the instability growth rate of the perturbation. If δ contains a real part, it is indicated that the solution $\phi(\xi)$ is linearly unstable, otherwise, $\phi(\xi)$ is linearly stable. In the following, we solve the linear eigenvalue problem (6).

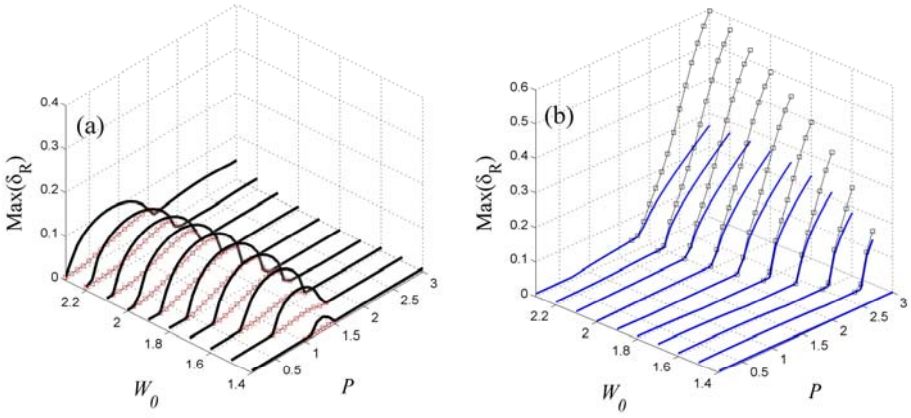

Fig. 4 – Eigenvalues of linear stability analysis: a) the largest real part of δ for SS1 (black solid curves) and AS1 (red rhombuses curves); b) the largest real part of δ for SS2 (blue solid curves) and AS2 (black squares curves). Here, the parameters are the same as in Fig. 3.

Figure 4 presents the dependence of the largest real part max(δ_R) of the symmetric and asymmetric solutions on the soliton power P and the modulation strength W_0. The solution is linearly stable for $\delta = 0$, otherwise, it is linearly unstable. In Fig. 4a, the largest real part of δ for SS1 and AS1 are plotted with black solid curves and red curves with rhombuses, respectively. The values of max(δ_R) for SS1 are larger than the ones for AS1 in their existence region, which indicates that the fundamental asymmetric soliton solutions are more stable than fundamental symmetric ones. The largest real part of max(δ_R) for SS2 and AS2 are displayed with blue solid curves and black squares curves in Fig. 4b. Obviously, the excited states of symmetric and asymmetric soliton solutions are all unstable in the existence region of AS2. It is interesting to compare Fig. 4 and Fig. 3; one can find that the fundamental and excited states of asymmetric soliton solutions always exist in that regions where the symmetric soliton solutions turn into unstable region, which indicates that the above mentioned special class of PT-symmetric potential is only a necessary condition for the symmetry-breaking bifurcations. Furthermore, the asymmetric soliton solutions could be induced by the unstable symmetric solitons.

The results of linear stability analysis for soliton solutions are further confirmed by employing direct numerical simulations of Eq. (2). The results are summarized in Fig. 5, in which the eigenvalue spectra of Eq. (6) for fundamental symmetric and asymmetric solutions are shown in panels (a_1) and (b_1), whereas the eigenvalue spectra of linear stability analysis of the excited states for the symmetric and asymmetric solutions are displayed in panels (c_1) and (d_1). The profiles of these soliton solutions can be seen in Fig. 1c and Fig. 1d, and Fig. 2c and Fig. 2d, respectively. We notice that both fundamental and excited state soliton solutions are linearly unstable. The eigenvalue spectra of the symmetric solitons appear in quartets, as shown in Fig. $5a_1$ and Fig. $5c_1$; however, this contrasts the asymmetric soliton solutions, see Fig. $5b_1$ and Fig. $5d_1$. Although the results of linear stability analysis show that these solutions must be unstable, these instabilities are relatively weak due to the small growth rates, which means that the corresponding oscillatory instabilities will be developed during a certain propagation distance ζ; the corresponding evolutions are displayed in $5a_2$, $5b_2$, $5c_2$, and $5d_2$.

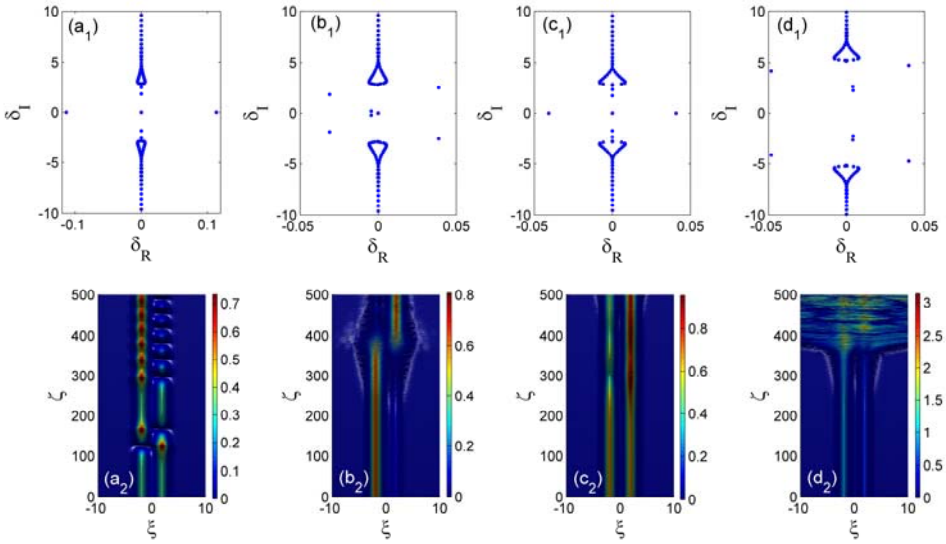

Fig. 5 – The eigenvalue spectra of linear stability analysis for the soliton solutions and the corresponding evolution plots: a_1), b_1), c_1) and d_1) the eigenvalue spectra of linear stability analysis for SS1 and AS1 with the soliton power 1.1, and for SS2 and AS2 with the soliton power 2.1, respectively; a_2), b_2), c_2), and d_2) the corresponding evolution plots of the field intensity. Here the other parameters are the same as in Fig. 1.

4. CONCLUSIONS

We have performed a systematic study of the symmetry breaking of solitons in PT-symmetric optical waveguides with competing cubic-quintic nonlinearity. The results have shown that the branches of asymmetric soliton solutions bifurcate from the base branches of PT-symmetric fundamental soliton and the excited state soliton solutions when increasing the input power. For the fundamental asymmetric soliton solutions, the eigenvalue spectrum begins to separate out and crosses the base branch of SS1, then ceases to exist and coalesces into the base branch again. However, for the excited state of asymmetric soliton solutions, the symmetry breaking bifurcations form the typical fork-type eigenvalue spectra structure. The effect of the modulation strength of PT-symmetric potential on the structure of eigenvalue spectra diagrams of the symmetric and asymmetric soliton solutions are investigated. We found that the region of the existence for asymmetric soliton solutions is intimately related to the stability of the symmetric soliton solutions. The stability of the symmetric and asymmetric soliton solutions is comprehensively analyzed by employing linear stability analysis and the different instability scenarios of solitons have also been revealed by using direct numerical simulations. The evolution plots indicate that the amplitudes of soliton solutions oscillate during a certain propagation distance due to the presence of weak instabilities.

ACKNOWLEDGEMENTS

This work was supported by Doctoral Scientific Research Foundation of Taiyuan Normal University No. I170144.

REFERENCES

1. C.M. BENDER, S. BOETTCHER, *Real Spectra in Non-Hermitian Hamiltonians Having PT Symmetry*, Phys. Rev. Lett., **80**, pp. 5243–5246, 1998.
2. C.M. BENDER, D.C. BRODY, H.F. JONES, *Complex Extension of Quantum Mechanics*, Phys. Rev. Lett., **89**, 270401, 2002.
3. C.M. BENDER, S. BOETTCHER, P.N. MEISINGER, *PT-symmetric quantum mechanics*, J. Math. Phys. **40**, pp. 2201–2229, 1999.
4. R. El-GANAINY, K.G. MAKRIS, D.N. CHRISTODOULIDES, Z.H. MUSSLIMANI, *Theory of coupled optical PT-symmetric*

structures, Opt. Lett., **32**, pp. 2632–2634, 2007.
5. S. KLAIMAN, U. GÜNTHER, N. MOISEYEV, *Visualization of Branch Points in PT-Symmetric Waveguides*, Phys. Rev. Lett., **101**, 080402, 2008.
6. V.S. BAGNATO, D.J. FRANTZESKAKIS, P.G. KEVREKIDIS, B.A. MALOMED, D. MIHALACHE, *Bose-Einstein Condensation: Twenty Years After*, Rom. Rep. Phys., **67**, pp. 5–50, 2015.
7. H. ALAEIAN, J.A. DIONNE, *Non-Hermitian nanophotonic and plasmonic waveguides*, Phys. Rev. B, **89**, 075136, 2014.
8. H. ALAEIAN, J.A. DIONNE, *Parity-time-symmetric plasmonic metamaterials*, Phys. Rev. A, **89**, 033829, 2014.
9. N. LAZARIDES, G.P. TSIRONIS, *Gain-Driven Discrete Breathers in PT-Symmetric Nonlinear Metamaterials*, Phys. Rev. Lett., **110**, 053901, 2013.
10. N.M. CHTCHELKATCHEV, A.A. GOLUBOV, T.I. BATURINA, V.M. VINOKUR, *Stimulation of the Fluctuation Superconductivity by PT Symmetry*, Phys. Rev. Lett., **109**, 150405, 2012.
11. A. RUSCHHAUPT, F. DELGADO, J.G. MUGA, *Physical realization of PT-symmetric potential scattering in a planar slab waveguide*, J. Phys. A: Math. Gen., **38**, pp. L171–L176, 2005.
12. A. GUO *et al*., *Observation of PT-Symmetry Breaking in Complex Optical Potentials*, Phys. Rev. Lett., **103**, 093902, 2009.
13. C.E. RÜTER *et al*., *Observation of parity-time symmetry in optics*, Nat. Phys., **6**, pp. 192–193, 2010.
14. T. KOTTOS, *Broken symmetry makes light work*, Nat. Phys., **6**, p. 166, 2010.
15. Z.H. MUSSLIMANI, K.G. MAKRIS, R. EL-GANAINY, D.N. CHRISTODOULIDES, *Optical Solitons in PT Periodic Potentials*, Phys. Rev. Lett., **100**, 030402, 2008.
16. F.KH. ABDULLAEV, Y.V. KARTASHOV, V.V. KONOTOP, D.A. ZEZYULIN, *Solitons in PT -symmetric nonlinear lattices*, Phys. Rev. A, **83**, 041805(R), 2011.
17. X. ZHU, H. WANG, L. ZHENG, H. LI, Y. HE, *Gap solitons in parity-time complex periodic optical lattices with the real part of superlattices*, Opt. Lett., **36**, pp. 2680–2682, 2011.
18. H. LI, Z. SHI, X. JIANG, X. ZHU, *Gray solitons in parity-time symmetric potentials*, Opt. Lett., **36**, pp. 3290–3292, 2011.
19. S. HU, X. MA, D. LU, Z. YANG, Y. ZHENG, W. HU, *Solitons supported by complex PT-symmetric Gaussian potentials*, Phys. Rev. A, **84**, 043818, 2011.
19. B. MIDYA, R. ROYCHOUDHURY, *Nonlinear localized modes in PT-symmetric Rosen-Morse potential wells*, Phys. Rev. A, **87**, 045803, 2013.
20. S. NIXON, L. GE, J. YANG, *Stability analysis for solitons in PT-symmetric optical lattices*, Phys. Rev. A, **85**, 023822, 2012.
21. D.A. ZEZYULIN, V.V. KONOTOP, *Nonlinear modes in the harmonic PT-symmetric potential*, Phys. Rev. A, **85**, 043840, 2012.
22. V. ACHILLEOS, P.G. KEVREKIDIS, D.J. FRANTZESKAKIS, R. CARRETERO-GONZÁLEZ, *Dark solitons and vortices in PT-symmetric nonlinear media: From spontaneous symmetry breaking to nonlinear PT phase transitions*, Phys. Rev. A, **86**, 013808, 2012.
23. M.A. MIRI, A.B. ACEVES, T. KOTTOS, V. KOVANIS, D.N. CHRISTODOULIDES, *Bragg solitons in nonlinear PT-symmetric periodic potentials*, Phys. Rev. A, **86**, 033801, 2012.
24. H. XU *et al*., *Nonlinear PT-Symmetric Models Bearing Exact Solutions*, Rom. J. Phys., **59**, pp. 185–194, 2014.
25. Y. HE, X. ZHU, D. MIHALACHE, *Dynamics of spatial solitons in parity-time-symmetric optical lattices: A selection of recent theoretical results*, Rom. J. Phys., **61**, pp. 595–613, 2016.
26. P. LI, B. LIU, L. LI, D. MIHALACHE, *Nonlinear parity-time-symmetry breaking in optical waveguides with complex Gaussian-type potentials*, Rom. J. Phys., **61**, pp. 577–594, 2016.
27. D. MIHALACHE, *Multidimensional localized structures in optical and matter-wave media: A topical survey of recent literature*, Rom. Rep. Phys., **69**, 403, 2017.
28. J. YANG, *Symmetry breaking of solitons in one-dimensional parity-time-symmetric optical potentials*, Opt. Lett., **39**, pp. 5547–5550, 2014.
29. J. YANG, *Can Parity-Time-Symmetric Potentials Support Families of Non-Parity-Time-Symmetric Solitons?*, Stud. Appl. Math., **132**, pp. 332–353, 2014.
30. J. YANG, *Symmetry breaking of solitons in two-dimensional complex potentials*, Phys. Rev. E, **91**, 023201, 2015.
31. H. CHEN, S. HU, *The asymmetric solitons in two-dimensional parity-time-symmetric potentials*, Phys. Lett. A, **380**, pp. 162–165, 2016.
32. P.F. LI, D. MIHALACHE, L. LI, *Asymmetric solitons in parity-time-symmetric double-hump Scarff-II potentials*, Rom. J. Phys., **61**, pp. 1028–1039, 2016.

Received August 31, 2017